ELSEVIER Journal of Electron Spectroscopy and Related Phenomena 114–116 (2001) 1127–1132

JOURNAL OF ELECTRON SPECTROSCOPY and Related Phenomena

www.elsevier.nl/locate/elspec

A theoretical investigation of photoemission spectra from $(GaAs)_2(AlAs)_2$ superlattices

T. Strasser[a], C. Solterbeck[a], W. Schattke[a,*], I. Bartoš[b], M. Cukr[b], P. Jiříček[b], C.S. Fadley[c], M.A. Van Hove[d]

[a]*Institut für Theoretische Physik und Astrophysik, Christian-Albrechts-Universität, Leibnizstr. 15, D-24098 Kiel, Germany*
[b]*Institute of Physics, Academy of Sciences of the Czech Republic, Cukrovarnika 10, 16253 Prague 6, Czech Republic*
[c]*Materials Sciences Division, Lawrence Berkeley National Laboratory, Berkeley, CA 94720, USA*
[d]*Department of Physics, University of California, Davis, CA 95616, USA*

Received 8 August 2000; received in revised form 3 October 2000; accepted 3 October 2000

Abstract

We calculated photoemission spectra within the one-step model for the (001) surface of the $(AlAs)_2(GaAs)_2$ superlattice structure. The purpose is to discriminate between spectral features which are caused by the surface, and those which are characteristic properties of the superlattice. Direct transitions indicate the opening of band gaps at the Brillouin zone edge, which are characteristic for the modified periodicity of the superlattice. Furthermore, the layer resolved photocurrent shows that one can also identify excitations from AlAs which are hidden below the first two GaAs layers and from As atoms at the boundary between the different semiconductors. Furthermore, emissions from surface states and resonances are also recognized.

Keywords: Superlattices; III/V Semiconductors; Photoemission; One-step model

1. Introduction

Superlattices are one important approach to band engineering and they are widely recognized for their unique electronic and optical properties. Because of their nearly equal lattice constants, GaAs and AlAs are suitable semiconductors for the creation of superlattices, e.g., by molecular beam epitaxy techniques. The electronic structure of the resulting superlattices cannot be treated as a simple spatial sequence of the band structures of the separate semiconductors. Already the larger periodicity perpendicular to the surface changes the symmetry of the Brillouin zone. This results in a back folding of the valence bands of the bulk material, which opens additional gaps at the edges of the Brillouin zone.

Photoemission spectroscopy is widely used to examine the electronic structures of materials. The spectra give insight into the valence band structure of the bulk as well as of the surface. Beside the initial states, photoemission involves the excitation to outgoing scattering states. Therefore, the bulk features are superposed with surface emissions and a full account of experimental data can only be attained by a comparison with photocurrents calculated within

*Corresponding author. Tel.: +49-431-880-4116.
E-mail address: schattke@tp.cau.de (W. Schattke).

0368-2048/01/$ – see front matter
PII: S0368-2048(00)00307-8

the one-step model of photoemission theory. Furthermore, the escape depth of photoelectrons is on the order of several Ångstroms. This leads to the question how the bulk superlattice periodicity influences the spectra obtained by photoemission.

The article is structured as follows. After a short overview about the theory, we present our results for the (001) surface of a $(AlAs)_2(GaAs)_2$ superlattice. The bulk band structure and the layer and orbital resolved density of states give an impression of the electronic properties of the crystal and its surface. Both are used for the interpretation of the calculated spectra in normal emission. In addition, layer resolved photocurrents are shown, which provide information about the origin of excitations.

2. Theory

The photocurrent is calculated within the one-step model. For details see the references [1,2]. In this 'Golden rule' formulation of the photoemission process the photocurrent I at the photon energy $h\nu$ is given by:

$$I \sim \sum_{i,j} \langle \Phi^*_{\mathrm{LEED}}(E_{\mathrm{fin}},k_\parallel)|\mathbf{A_0}\cdot\mathbf{p}|\Psi_i\rangle \; G_{i,j}(E_{\mathrm{fin}}-h\nu,k_\parallel)\langle\Psi_j|\mathbf{p}\cdot\mathbf{A_0}|\Phi^*_{\mathrm{LEED}}(E_{\mathrm{fin}},k_\parallel)\rangle.$$

The vector potential of the light $\mathbf{A_0}$ is kept constant, $\mathbf{p}$ denotes the momentum operator and $k_\parallel$ is the parallel momentum. The initial states are represented by a half-space Green's function. This Green's function $G_{i,j}$ is given in a layer resolved linear combination of atomic orbitals Ψ_i. Our basis set consists of the 4s and 4p atomic orbitals of gallium and arsenic and the 3s and 3p atomic orbitals of aluminum. The associated Hamilton matrix is calculated according to the Extended Hückel Theory [3,4]. In this theory a small number of parameters is used to determine the hamilton matrix $\hat{H}(\vec{k})$ in a basis of atomic orbitals from the calculated matrix of orbital overlaps $S(\vec{k})$ as a function of Bloch vector $\vec{k}$. The parameters for GaAs and AlAs are listed in Refs. [3,4]. Because they should be used to describe a heterostructure, we slightly modify the parameters. They are adjusted to the band offset between GaAs and AlAs of 0.45 eV [8]. The parameters as finally used are given in Table 1. The electronic structure of the surface is determined by the calculation of the $k_\parallel$ resolved density of states (DOS) from the half-space Green's matrix $G_{i,j}$, the same as used for the photocurrent. The Green's matrix is calculated by a highly convergent renormalization scheme [6], which takes into account relaxation and reconstruction at the surface.

The final state of photoemission is a time reversed LEED-state Φ^*_{LEED} with final state energy E_{fin}. Its wave function is determined by matching the solution of the complex band structure to the vacuum solution, representing the surface by a step potential. The solution within the bulk is calculated by the empirical pseudopotential method, as described by Mäder and Zunger [7]. They developed a method which permits specifying the form factors for continuous reciprocal lattice vectors and tested them for GaAs and AlAs. The damping of the final state wave function inside the crystal is described by the imaginary part of an optical potential.

In this examination, two different descriptions of the Hamiltonian for the initial and the final states are used. Such a distinction is necessary to account for the different selfenergies. Technically, it takes into account the difference in the localization of the electrons in the initial and final states. Furthermore, the tight-binding description provide a simple ap-

Table 1
EHT-parameter for GaAs and AlAs (for the notation see Starrost et al. [3,4])

Atom	K_{ss}	K_{sp}	K_{pp}	I_s	I_p	$\tilde{I}_s$	$\tilde{I}_p$
As (GaAs)	1.000	0.844	0.844	39.38	22.50	16.46	8.53
Ga (GaAs)	1.000	0.844	0.844	24.38	22.50	15.24	8.53
As (AlAs)	1.000	0.750	0.563	20.63	28.13	9.42	8.81
Al (AlAs)	1.000	0.750	0.563	30.00	39.38	19.17	10.03

proach for the orbital resolved density of states, which is an important tool in the interpretation of photoemission spectra.

3. Results and discussion

In this section we present our results for a $(AlAs)_2(GaAs)_2(001)$–(1×1)Ga surface. The surface geometry is shown in Fig. 1, where also a schematic side view of the superlattice is given. The superlattice consists of a periodic sequence of two GaAs and two AlAs layers, respectively, which starts with GaAs at the surface. The surface itself is a Ga terminated continuation of the bulk structure. Fig. 2 shows the bulk band structure for the $(AlAs)_2(GaAs)_2$ superlattice in the ΓZ direction. This direction is relevant for photoemission in normal emission from the (001) surface. For the superlattice the symmetry of the Brillouin zone changes from face-centered cubic for, e.g., GaAs to tetragonal. The length between Γ and Z corresponds to one-quarter of the original ΓX distance. For a better comparison also the bulk band structure of GaAs for the ΓX direction is plotted (thin lines). A first impression of the resulting band structure for the superlattice can be obtained by back folding of the bulk valence bands into the smaller Brillouin zone,

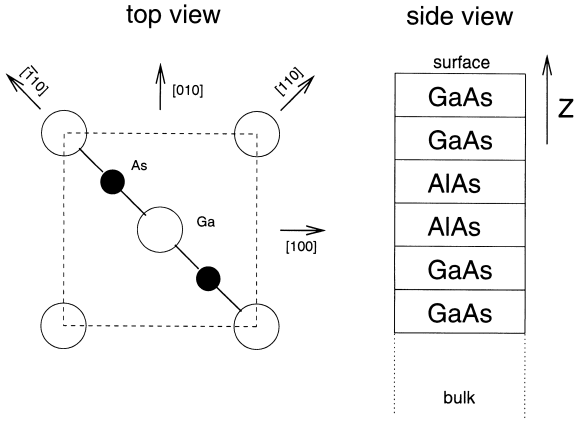

Fig. 1. Assumed ideal geometry of $(AlAs)_2(GaAs)_2(001)$–(1×1)Ga surface (left side) and schematical side view of superlattice (right side). Gallium atoms of first layer are shown as open circles, arsenic atoms of second layer as filled circles.

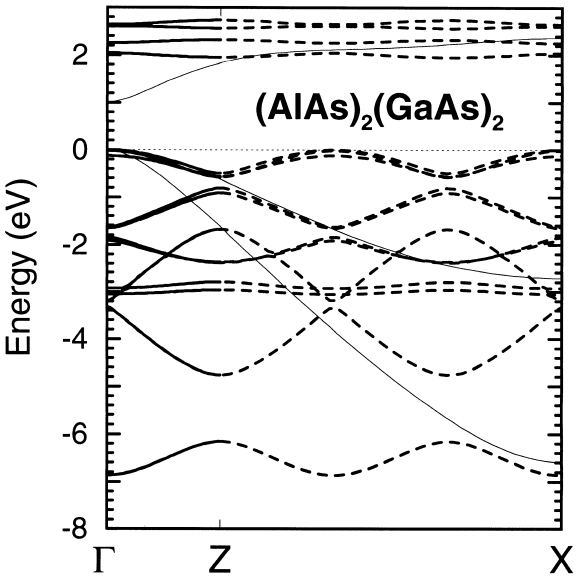

Fig. 2. Bulk band structure for $(AlAs)_2(GaAs)_2$ superlattice. Real Brillouin zone terminates at Z, bands are continued up to X point. Bulk band structure of GaAs is plotted by thin solid lines.

together with the opening of band gaps at their edges. A comparison between both band structures shows that the band width of the superlattice is comparable to that of bulk GaAs but that the fundamental gap increases by about 1 eV. Furthermore, we recognize the opening of the band gaps for the superlattice at the edge of the Brillouin zone near Z, particular near -6.0 eV binding energy. The band structure can be compared to results from Gopalan et al. [5]. In their calculation, the band structure shows a gap near -6.0 eV, which has half the width of that in this work. Furthermore, the results of Gopalan et al. include a band between -0.3 and -1.2 eV, which is more dispersive than its counterpart in this work. Apart from this, the two calculations show a reasonable agreement up to -7 eV binding energy.

Fig. 3 shows the density of states (DOS), which is calculated for the Γ point. This high symmetry point is of central interest for an understanding of photoemission in normal emission. The orbital resolved density of states exhibits a strong surface state at -6.0 eV, which consists of contributions of gallium s orbitals and also weak contributions from As and Ga p_z orbitals. This surface state is located in the

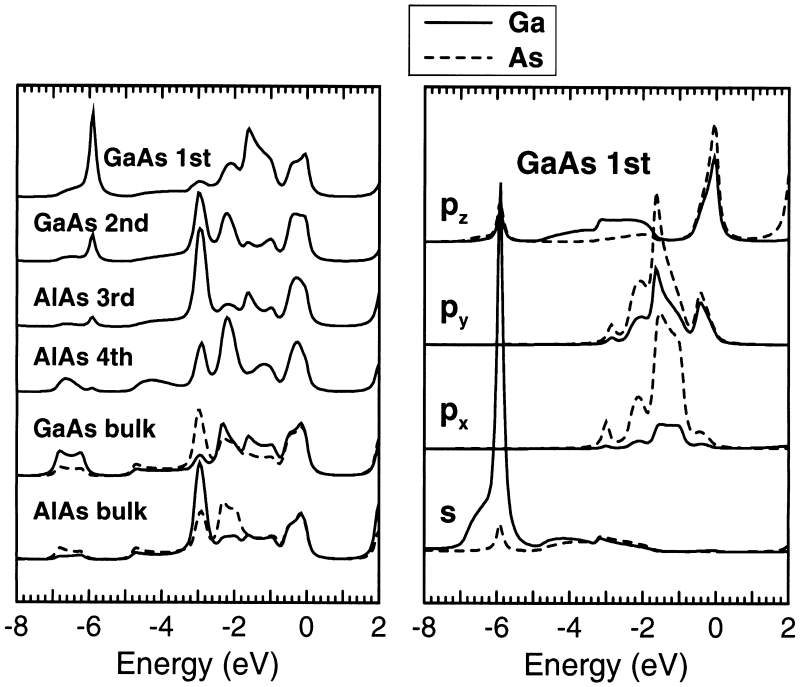

Fig. 3. Density of states for $(AlAs)_2(GaAs)_2(001)$–(1×1)Ga surface at $\bar{\Gamma}$ point. On left hand side DOS is resolved by layers, on right hand side DOS of first GaAs bilayer is resolved by atoms and orbitals.

additional band gap, which opens near −6.0 eV (see Fig. 2). This band gap can be seen as a depression in the bulk-DOS on the left hand side of Fig. 3. The surface state has a tail into the crystal, which can be followed up to the fourth AlAs layer. Near the valence band maximum (VBM), strong contributions from Ga and As p_z orbitals are found. Being resonances they are related to a dangling bond state, which becomes a clear surface state, when continued into the surface Brillouin zone (not shown). At higher binding energies, the density of states is dominated by As p_x and p_y orbitals, with lower contributions from their Ga counterparts. Between −2.0 and −5.0 eV binding energy, also Ga p_z and s orbitals give rise to a broad structure in the DOS.

The spectra of Fig. 4 are for normal emission with light incident in the [110] direction and polarized parallel to the plane which is spanned by the [110] direction and the *z*-axis. The polar angle of incidence is 45°. The position of the bars indicates transitions between initial and final bands with exact conservation of the perpendicular wave vector. In Fig. 4 transitions only to those bulk bands being dominant in the final state are marked. Near the lower valence band edge at −6.9 eV a weak dispersing structure (F) is thus observed. A second dispersive emission (D) is visible for binding energies between −2.4 and −4.8 eV. The two dispersive structures (D) and (F) mark the band gap at the Brillouin zone edge *Z* around −6.0 eV. The opening of this gap in the photoemission spectra is the characteristic property of the superlattice. The dispersionless structure (E) at −6.0 eV is caused by the Ga s and As p_z surface state, which was discussed in the context of Fig. 3 above. The surface emission (E) lies near the lower edge of the superlattice band gap. In the experiment, this vicinity could confuse the accurate identification of the gap width. The spectra show a second strong emission near 0 eV, which is more or less dispersionless. This emission is caused by the Ga and As p_z orbitals, see Fig. 3. Near 35.0 eV excitation energy, also direct transitions from the VBM contribute to structure (A). At higher binding energies of −2.2 and −3.0 eV, Fig. 4 presents the two nearly disper-

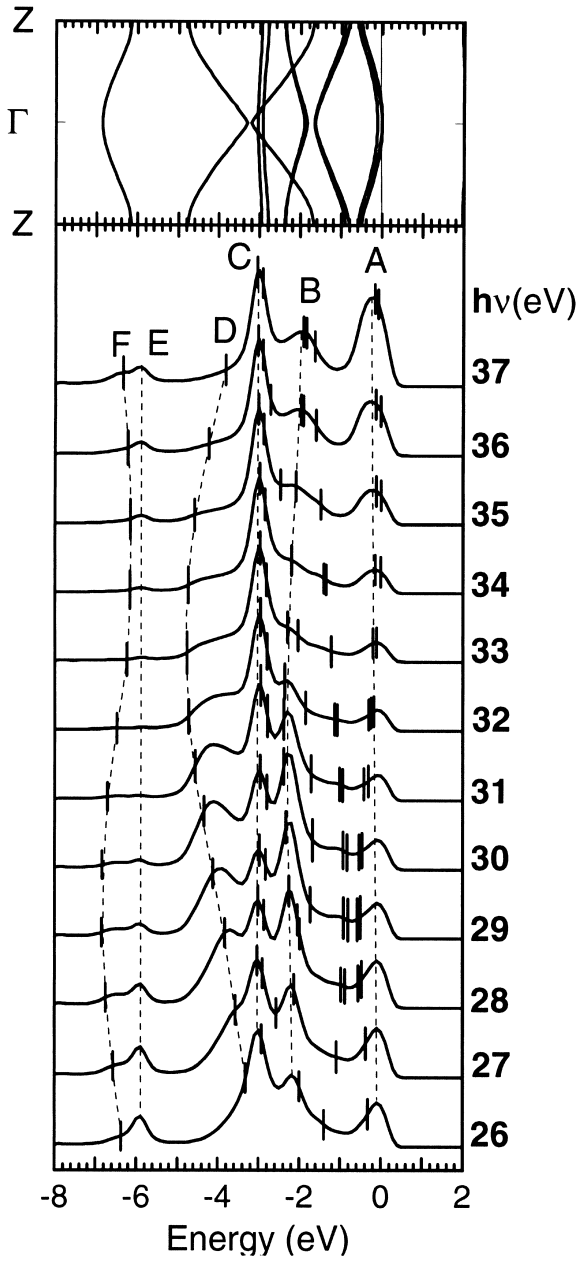

Fig. 4. Theoretical normal emission spectra for $(AlAs)_2(GaAs)_2(001)-(1\times1)Ga$. Bars indicate binding energies at which direct transitions would be expected. At top, bulk band structure is shown.

sionless structures (B) and (C). In this energy range, the DOS shows contributions mainly from the p_x and p_y orbitals of Ga, Al and As. Both structures are influenced by different direct transitions from the partly flat bands, which cross this region. Beyond this, the layer resolved photocurrent presents deeper insight into the compositions of the spectra.

Fig. 5 shows the layer resolved photocurrent for three selected photon energies (19.0, 24.0 and 27.0 eV). The thin solid line represents the total photocurrent calculated for nine double layers of alternating $(GaAs)_2$ with $(AlAs)_2$. The photocurrent for 19 eV excitation energy shows an increasing intensity of structure (B) (marked by an arrow) when considering first the surface, then introducing the layers below and finally all nine $(GaAs)_2(AlAs)_2$ layers, consistent with an expected direct transition from the bulk. For 24.0 eV this contribution to the photocurrent has its source in the AlAs layers, below the first double layer GaAs. For higher excitation energies, the emission from the first double layer GaAs increases. The structure (C) (see Fig. 4) shows a similar behavior. Beside direct transitions from the nearly dispersionless bulk bands around -3.0 eV, strong emissions from the As p_x orbitals, which flank the boundary between the first double layer of GaAs and of AlAs, could be identified. This applies especially for photon energies between 32.0 and 37.0 eV.

4. Conclusion

We calculated spectra of the angle resolved photoelectron spectroscopy for the (001) surface of a $(AlAs)_2(GaAs)_2$ superlattice. The analysis of the theoretical spectra points out that photoelectron spectroscopy is able to detect specific properties of the superlattice. The spectra in normal emission indicate the opening of a band gap at the Brillouin zone edge, which is caused by the periodicity of the superlattice. The use of layer-resolved photocurrents reveals the origin of excitations from AlAs even below the second layer GaAs and identifies emissions from the interface between both semiconductors involved. The contributions of single layers to the photocurrent are strongly dependent on the excitation energy. Beside these emissions which are characteristic for the superlattice, also emissions from a surface state, located inside the band gap and a surface resonance near the upper valence band edge are found and their orbital composition is

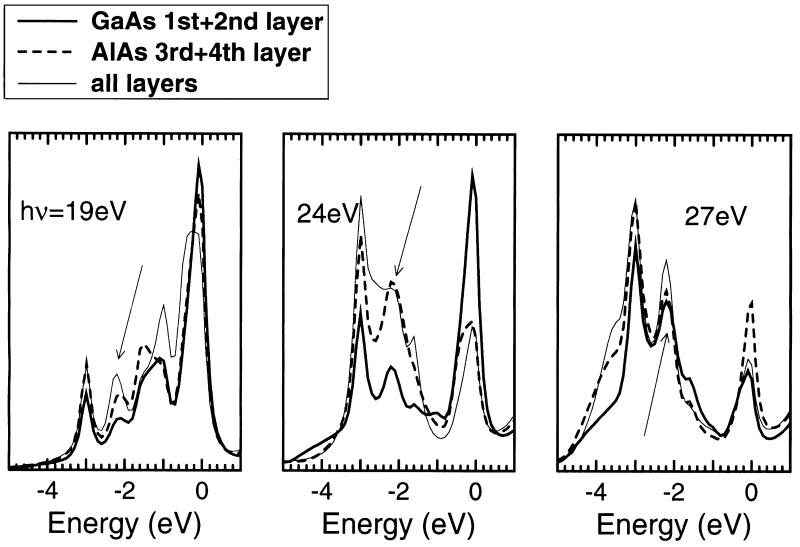

Fig. 5. Layer resolved photocurrent (normal emission) for $(AlAs)_2(GaAs)_2(001)-(1\times1)Ga$, calculated for three different photon energies. Spectra are not broadened with an experimental resolution and not multiplied by a Fermi distribution. Arrows mark structure (B) of Fig. 4. Thick solid lines: photocurrent from the first two GaAs bilayers; thick dotted lines: photocurrent integrated from the first two GaAs and AlAs bilayers; thin solid lines: photocurrent from all 36 bilayers, taken into account in the calculation.

evaluated. Thus, angle-resolved photoelectron spectroscopy might be a powerful tool for the investigation of superlattices, provided that detailed calculations within the one-step model are available as a reference.

Acknowledgements

The work was supported by the BMBF under contract no. 05 SB8 FKA7, and the DAAD under contracts nos. 315/PPP and TSR-075-97,as well as by NSF contract INT-9815358. It was supported in part by the Director, Office of Science, Basic Energy Sciences, Materials Sciences Division, of the US Department of Energy under Contract No. DE-AC03-76SF00098.

References

[1] J. Henk, W. Schattke, H.P. Barnscheidt, C. Janowitz, R. Manzke, M. Skibowski, Phys. Rev. B 39 (1989) 13286.
[2] J. Henk, W. Schattke, H. Carstensen, R. Manzke, M. Skibowski, Phys. Rev. B 47 (1993) 2251.
[3] F. Starrost, S. Bornholdt, C. Solterbeck, W. Schattke, Phys. Rev. B 53 (1996) 12549.
[4] F. Starrost, S. Bornholdt, C. Solterbeck, W. Schattke, Phys. Rev. B 54 (1996) 17226.
[5] E.T. Yu, D.H. Chow, T.C. McGill, Phys. Rev. B 38 (1988) 12764.
[6] J. Henk, W. Schattke, Comput. Phys. Commun. 77 (1993) 69.
[7] K.A. Mäder, A. Zunger, Phys. Rev. B 50 (1994) 17393.
[8] S. Gopalan, N.E. Christensen, M. Cardona, Phys. Rev. B 39 (1989) 5165.